Hybrid nanoantennas for directional emission enhancement

Evgenia Rusak, Isabelle Staude, Manuel Decker, Jürgen Sautter, Andrey E. Miroshnichenko, David A. Powell, Dragomir N. Neshev, and Yuri S. Kivshar

Citation: Applied Physics Letters **105**, 221109 (2014); doi: 10.1063/1.4903219
View online: http://dx.doi.org/10.1063/1.4903219
View Table of Contents: http://scitation.aip.org/content/aip/journal/apl/105/22?ver=pdfcov
Published by the AIP Publishing

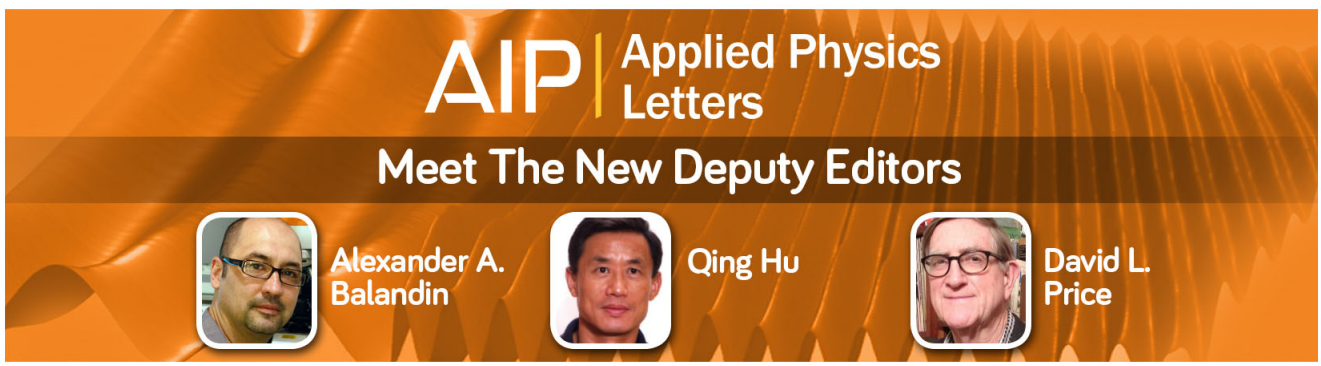

Hybrid nanoantennas for directional emission enhancement

Evgenia Rusak, Isabelle Staude,[a] Manuel Decker, Jürgen Sautter,
Andrey E. Miroshnichenko, David A. Powell, Dragomir N. Neshev, and Yuri S. Kivshar
Nonlinear Physics Centre and Centre for Ultrahigh Bandwidth Devices for Optical Systems (CUDOS), Research School of Physics and Engineering, The Australian National University, Canberra, ACT 2601, Australia

(Received 22 October 2014; accepted 19 November 2014; published online 4 December 2014)

Plasmonic and dielectric nanoparticles offer complementary strengths regarding their use as optical antenna elements. While plasmonic nanoparticles are well-known to provide strong decay rate enhancement for localized emitters, all-dielectric nanoparticles can enable high directivity combined with low losses. Here, we suggest a hybrid metal-dielectric nanoantenna consisting of a gold nanorod and a silicon nanodisk, which combines all these advantages. Our numerical analysis reveals a giant enhancement of directional emission together with simultaneously high radiation efficiency (exceeding 70%). The suggested hybrid nanoantenna has a subwavelength footprint, and all parameters and materials are chosen to be compatible with fabrication by two-step electron-beam lithography. © *2014 AIP Publishing LLC*. [http://dx.doi.org/10.1063/1.4903219]

Owing to their ability to efficiently couple localized optical near-fields to propagating light waves, optical nanoantennas remain a current focus of nanophotonics research.[1] In particular, they have been shown to allow for directional emission enhancement from a localized nanoemitter,[2–6] a key functionality in the context of next generation light sources, including on-chip integrated sources,[7] efficient quantum-light sources,[8] and display technology. While most nanoantennas consist of metallic nanoparticles supporting localized surface plasmons, resonant dielectric nanoparticles are rapidly becoming a paradigm of nanoantenna design, propelled by their very low optical losses as compared to nanoplasmonic structures.[9,10] In addition, high-index all-dielectric nanoparticles exhibit both electric and magnetic multipolar resonances, whose engineered far-field interference offers unique opportunities for creating highly directional radiation patterns with near-unity radiation efficiency.[11–13]

However, the maximum radiative decay rate enhancement expected for single-particle all-dielectric nanoantennas does not match the large values demonstrated for plasmonic enhancement.[1,14] Thus, in order to combine the respective advantages of plasmonic and all-dielectric nanoantennas, metal-dielectric composites have been suggested.[15–17] In such hybrid nanoantennas, a metallic nanoparticle is used as a *feed element*, providing a high radiative decay rate enhancement, while an all-dielectric nanoparticle is employed as a *director element*, shaping the nanoantenna's emission into a unidirectional pattern without the addition of appreciable losses. However, high directivity, high efficiency, and subwavelength dimensions have not yet been simultaneously achieved by hybrid nanoantennas. Most importantly, hybrid nanoantenna designs that are accessible by well-controlled top-down fabrication schemes are still missing.

In this letter, we study numerically hybrid nanoantennas that employ gold nanorods as feed elements and a silicon nanodisk as a director element. All structure parameters are chosen to be compatible with fabrication *via* two-step electron-beam lithography, and the constituent materials are limited to gold, silicon, and silica glass, which are commonly used in optical nanofabrication. Also, the dimensions of the hybrid structure are well below the free-space operation wavelength of the nanoantenna in all three dimensions. We perform comprehensive numerical analyses of the suggested nanoantenna design, assessing its actual performance for key applications of directional nanoantennas.

A sketch of the considered geometry is shown in Fig. 1. A gold nanorod—which was chosen because it is a well studied nanoantenna element[1,18]—serves as a feed element. The width W and thickness T of the gold rod are both set to 40 nm. The length L of the rod is 172 nm, resulting in a resonance wavelength of the gold rod of 1.111 μm. To avoid unphysically sharp edges, we model the gold nanorod edges

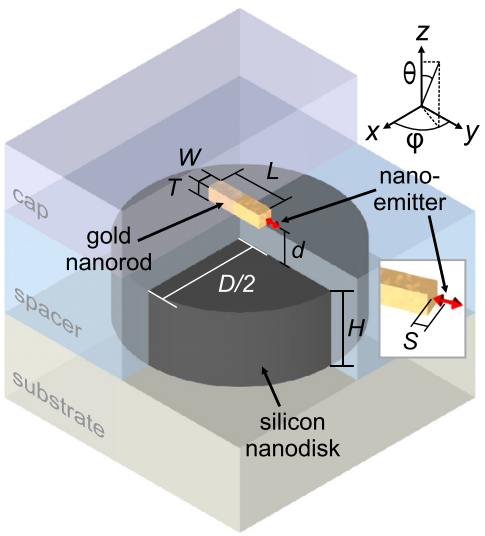

FIG. 1. Schematic of a hybrid nanoantenna: The emission from a dipole emitter (red double-arrow) is enhanced by a gold nanorod and redirected by a silicon nanodisk.

[a]Author to whom correspondence should be addressed. Electronic mail: isabelle.staude@anu.edu.au

as rounded with a radius of curvature of 10 nm. A silicon nanodisk acts as a director element. The diameter D of the nanodisk is 620 nm, and its height, H, is 220 nm. The distance between the gold nanorod and the surface of the silicon nanodisk is denoted by d. The gold and silicon optical properties are modeled using experimental data from Refs. 19 and 20, respectively.

A possible fabrication scheme for this hybrid nanoantenna would involve a first step of electron-beam lithography on a silicon thin-film on a glass substrate of macroscopic thickness, followed by reactive ion etching in order to define the silicon nanodisk director element.[13] Next, a silicon oxide layer can be deposited onto the silicon nanodisk. Control of the thickness of this layer provides control over the separation distance d. The gold nanorod acting as a feed element can then be defined in a second step of electron-beam lithography followed by evaporation of a thin layer of gold and a lift-off procedure. As a last step, application of an index-matched cap layer can be used to embed the hybrid nanoantenna into a homogeneous medium. Based on this suggested fabrication scheme, in our calculations, we approximate the entire hybrid nanoantenna as embedded into a homogeneous medium formed by the substrate, the spacer layer, and the cap, with an refractive index of $n = 1.45$ corresponding to silica glass. While—for an experimentally fabricated structure—a slight residual refractive index mismatch between the layers may occur, it can be kept very small, not noticeably impacting on the nanoantenna performance.

We consider the hybrid nanoantenna to be excited by a nanoemitter, e.g., an atom or a quantum dot. The nanoemitter is modeled as a point-like broadband dipole source and displayed as a red double-arrow in Fig. 1, corresponding to the dipole axis. It is aligned parallel to the main axis of the gold nanorod and perpendicular to the symmetry axis of the nanodisk. The distance S from the surface of the gold rod to the center of the nanoemitter is set to 6.5 nm. A number of previous studies have concentrated on characterizing the emission characteristics of coupled systems consisting of a dipole emitter and a plasmonic nanoantenna as a function of both the orientation of the dipole with respect to the gold nanorod as well as the distance between the nanoemitter and the gold nanorod.[21] Here, we have directly chosen these parameters in order to optimize the radiative decay rate enhancement provided by the feed element. It is worth noting that a higher total decay rate enhancement can be achieved if the distance between the emitter and the plasmonic particle S is further reduced, however, the radiation efficiency would decrease due to quenching, leading to a reduction of the radiative decay rate enhancement.[21] All calculations are performed using the commercially available software package CST Microwave Studio.

We start our analysis from a simpler structure consisting of a silicon nanodisk excited by a point-like dipole source. Such structures have been suggested to provide large front-to-back ratio and high directivity.[13] Here, we start by revisiting the key properties of such element. The directivity of an antenna $D_A(\theta,\phi)$ is defined as

$$D_A(\theta,\phi) = \frac{4\pi U_A(\theta,\phi)}{\int_0^{2\pi}\int_0^{\pi} U_A(\theta,\phi)\sin(\theta)\,d\theta\,d\phi}, \qquad (1)$$

where $U_A(\theta,\phi)$ is the radiation intensity in a given direction with respect to the antenna.[22] Figure 2(a) shows the calculated directivity in forward direction $D_0 = D_A(0, 0)$ (red line) of a single nanodisk with the above specified dimensions. The excitation dipole source is oriented along y-direction and located at 80 nm away from the nanodisk surface at its symmetry axis. The directivity reaches its maximum of 7.6 at the operation wavelength of $\lambda = 1.111\ \mu$m. Also shown are the total power radiated by the nanodisk antenna (blue line) and, for comparison, by the exciting dipole source alone (black dashed line). Note that, despite the high directivity of the nanodisk antenna, its total radiated power at the operation wavelength is in fact reduced in comparison to that of the dipole source alone, which immediately pinpoints the need for hybridization of this nanoantenna with a plasmonic element, if radiative decay rate enhancement is desired. In order to investigate the origin of the highly directive behavior of the nanodisk antenna, we perform a multipole expansion[23] of the total scattering response of the silicon nanodisk, according to

$$C_{sca}^{disk} = \frac{\pi}{k^2}\sum_{l=1}^{\infty}\sum_{m=-l}^{l}(2l+1)\left[|a_{lm}|^2 + |b_{lm}|^2\right]. \qquad (2)$$

Such analyses are usually performed for plane-wave excitation.[13,24] In our case, however, in order to provide an accurate picture of our system, we consider the same dipole excitation scenario as before. The results for the non-negligible coefficients are presented in Fig. 2(b). Most interestingly, the a_{21} coefficient, corresponding to an electric quadrupole

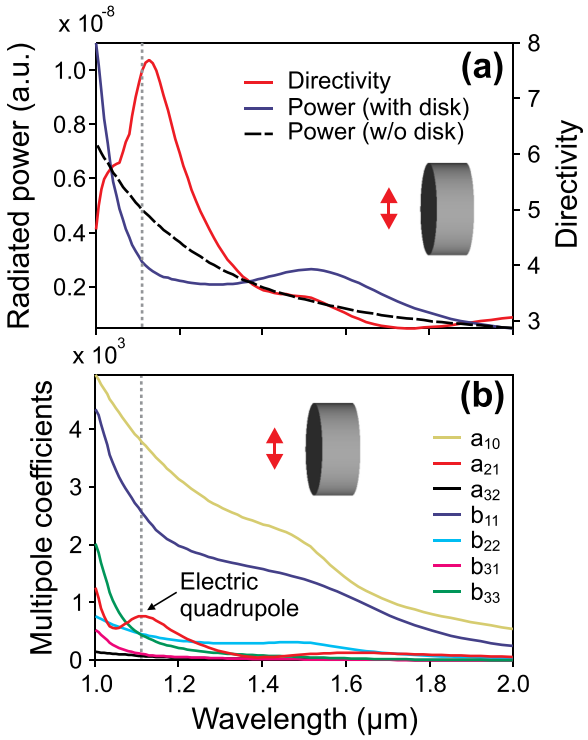

FIG. 2. (a) Total radiated power and directivity of a single silicon nanodisk excited by a point-like broadband dipole source. Also shown for comparison is the power radiated by the exciting dipole source alone. (b) Multipole expansion (see Eq. (2) for the definition of the plotted coefficients) of the total power radiated by the silicon nanodisk under dipole excitation. Only the non-negligible multipole coefficients are shown. The vertical dashed lines in (a) and (b) indicate the operation wavelength of $\lambda = 1.111\ \mu$m.

contribution, shows a resonant behaviour at the operation wavelength. This suggests that the electric quadrupole plays a crucial role for the functionality of this director element, enabling hybrid nanoantennas with directivities exceeding those of previously suggested subwavelength designs, where the functionality of the all-dielectric director element is based on the interference of the electric and magnetic dipole modes alone.[16] In accordance with our results, the interference of higher-order multipoles beyond the electric and magnetic dipole has been recently shown to dramatically improve the directionality of forward scattering.[6,10,25] Repeating our analysis for far-field excitation (not shown), we find that the contribution of the electric quadrupole becomes dominant at the operation wavelength, leading to a maximum of the total scattering cross-section.

Next, we turn our attention to the hybrid nanoantenna and investigate how variation of the distance between the gold nanorod and the surface of the silicon nanodisk d influences its characteristic quantities. To this end, we calculate the directivity in forward direction, the radiative decay rate enhancement, the radiation efficiency, and the directional emission enhancement for the variation of the distance between the gold nanorod and the silicon nanodisk. The directivity in forward direction $D_0 = D_A\,(0,0)$ is displayed in Fig. 3(a). This quantity strongly depends on the distance between the gold nanorod and the silicon disk and achieves higher values when the distance is increased starting from an initial value of 40 nm. The highest value of 7.7 is obtained at a distance of 90 nm for a wavelength of $\lambda = 1.124\,\mu$m, and it remains almost constant for distances in the range of 80 nm–100 nm.

The total emitted power P_{tot} of the nanoemitter and the radiated power P_{rad} of the emitter-nanoantenna coupled system are obtained by numerically calculating the power flow through a closed surface surrounding the nanoemitter at a distance of 1 nm and 800 nm, respectively. The radiative decay rate enhancement Γ_{rad} is given by the relationship $\Gamma_{rad} = P_{rad}/P_0$, where P_0 is the power emitted by the nanoemitter into a homogeneous $n = 1.45$ environment. Note that, in general, $P_{tot} \neq P_0$ due to the presence of the nanoantenna. The radiation efficiency is the ratio between the radiated power and the total emitted power: $e_0 = P_{rad}/(P_{rad} + P_{nr}) = P_{rad}/P_{tot}$. This quantity takes into account the non-radiative losses P_{nr} of the nanoantenna. The peak value of the radiative decay rate enhancement [see Fig. 3(b)] experiences a blue-shift when the distance d is increased which can be explained by a reduction of the effective refractive index in the vicinity of the gold nanorod. The maximum values of the radiative decay rate enhancement [see Fig. 3(b)] and of the radiation efficiency [see Fig. 3(c)], on the other hand, do not appear very sensitive to the variation of the distance between the gold nanorod and the silicon nanodisk.

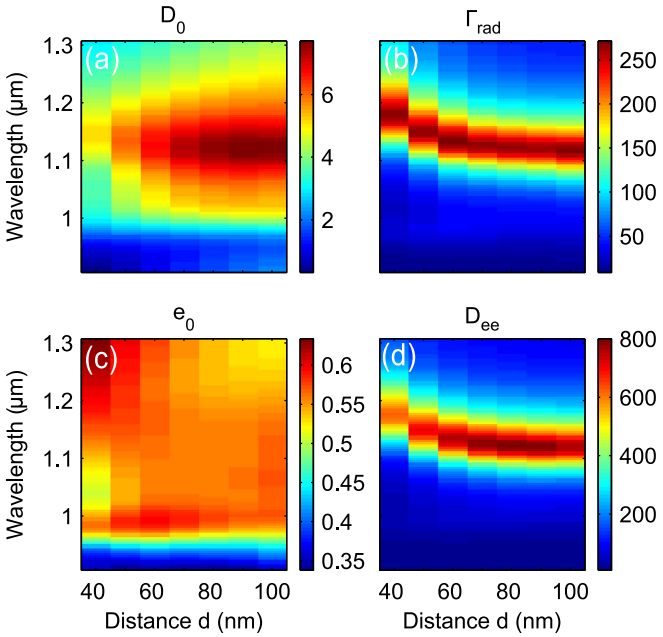

FIG. 3. (a) Directivity in forward direction D_0, (b) radiative decay rate enhancement Γ_{rad}, (c) radiation efficiency e_0, and (d) directional emission enhancement D_{ee} for a variation of the distance d between the gold nanorod and the silicon nanodisk.

Finally, we discuss the directional emission enhancement D_{ee}—a crucial quantity for the actual capability of the nanoantenna to enhance the brightness of a given nanoemitter in a standard microscope setup. It can be expressed as the product of the radiative decay rate enhancement Γ_{rad} and the enhancement of the collection efficiency due to directional emission, Γ_{col}, or equivalently as the ratio of the power radiated into a certain solid angle by the nanoemitter in the presence of the nanoantenna $U_A\,(\theta,\phi)$ to its emitted power in a homogeneous $n = 1.45$ environment $U_E\,(\theta,\phi)$ for the optimal dipole orientation

$$D_{ee} = \Gamma_{rad} \times \Gamma_{col} = \frac{\int_0^{2\pi}\int_0^{\theta_0} U_A(\theta,\phi)\sin(\theta)\mathrm{d}\theta\mathrm{d}\phi}{\int_0^{2\pi}\int_0^{\theta_0} U_E(\theta,\phi)\sin(\theta)\mathrm{d}\theta\mathrm{d}\phi}. \quad (3)$$

Importantly, this definition accounts for non-radiative losses in the metallic nanorod. We choose the solid angle over which the integrals are calculated to be limited by the angle of total internal reflection, which is given by $\theta_0 = \sin^{-1}(1/1.45) \approx 43.6^{\circ}$. In experiments, this corresponds to the fraction of the photoluminescence that can escape from the glass substrate without the use of immersion oil objectives. Note that for the suggested nanoantenna geometry, the direction of maximum directivity coincides with the normal of the substrate-air interface, thereby minimizing the fraction of emitted light that undergoes total internal reflection. We neglect partial reflection of light in our calculation of the directional emission enhancement considering that it can be strongly suppressed by an antireflection coating of the substrate. Similar to the directivity in forward direction, the directional emission enhancement is sensitve to the distance between the gold nanorod and the silicon nanodisk, reaching its maximum value of 800 for a distance $d = 80$ nm [see Fig. 3(d)]. The starting point for further optimization is that the radiative decay rate enhancement displayed in Fig. 3(b) is dominated by the properties of the feed element. Thus, it can be further increased through modification of the latter. To illustrate this possibility, we consider a variation of our hybrid geometry, where the single gold nanorod is replaced by two gold nanorods separated by a small feed gap [see insets in Fig. 4]. The nanoemitter is situated in the centre of

this feedgap and oriented as previously. We choose the gap as 30 nm to stay well within the fabrication limitations. The length L_{TR} of each rod is tuned to 150 nm resulting in a resonance wavelength of the gap nanoantenna of $\lambda = 1.111\ \mu$m; the width W and thickness T are the same as before. The distance d is set to the optimum value of 80 nm.

In Fig. 4, we compare the performance for the two hybrid nanoantenna designs. Results for the purely dielectric nanoantenna, consisting of the silicon disk alone, are also included for comparison. The directivity in the forward direction [see Fig. 4(a)] reaches its maximum value of 8.5 for the two rod nanoantenna at a wavelength of $\lambda = 1.091\ \mu$m. Note that this value is obtained for a homogenous dielectric environment and will likely be further enhanced by taking a substrate into account. Minor lateral misalignment of the gold nanorod with respect to the silicon nanodisk merely results in a slight deviation of the beaming direction from the symmetry axis of the structure while the high directivity is preserved. The highest values of radiative decay rate enhancement [see Fig. 4(b)] are also obtained for the case of the two rod nanoantenna, which can be explained by the higher electric-field enhancement in the feed-gap provided by the two rods compared to one.[1,18] Importantly, both hybrid geometries show much higher radiative decay rate enhancement than the silicon nanodisk alone, which does not provide an as large local electric-field enhancement as the metallic particles in the hybrid designs. The radiation efficiency e_0 [see Fig. 4(c)], on the other hand, is highest for the all-dielectric nanoantenna, since the silicon disk is practically non-absorbing in the wavelength range of interest. The radiation efficiency of the hybrid design with the two gold nanorods still reaches 70% over the entire wavelength range from 0.95 μm to 1.3 μm, again outperforming the single rod hybrid antenna.

Based on our results so far, we can furthermore compare the performance of the two rod hybrid nanoantenna to that of an ideal plasmonic Yagi-Uda nanoantenna in a homogeneous environment.[2] Indeed, both the directivity and the radiation efficiency of the hybrid nanoantenna are significantly higher. The gain in radiation efficiency originates from the replacement of lossy metallic director elements with a single loss-free silicon nanodisk. Finally, the high directivity and radiative decay rate enhancement of the two rod nanoantenna directly translate to a large directional emission enhancement D_{ee} [see Fig. 4(d)]: While—for the single rod hybrid nanoantenna—D_{ee} reaches an already high value of 800 at a wavelength $\lambda = 1.123\mu$m, a maximum of 1400 is achieved at $\lambda = 1.111\mu$m for the two rod hybrid antenna.

In conclusion, we have proposed and systematically investigated a hybrid metal-dielectric nanoantenna, where a single nanoemitter is coupled to a gold nanorod and the emission is redirected by a silicon nanodisk. We have compared this design with a single silicon nanodisk alone and also with a design where the single nanorod is replaced by a gap nanoantenna. In addition to a high directivity of 8.5 and high radiative decay rate enhancement typical for plasmonic gap nanoantennas, we have achieved a high radiation efficiency exceeding 70% over a broad wavelength range of more than 300 nm accompanied by strong directional emission enhancement of 1400. Our results indicate that the suggested hybrid nanoantenna combines the respective advantages of both plasmonic and all-dielectric nanoantennas. The dimensions and materials of the nanoantenna design are chosen to allow for fabrication by standard top-down nanofabrication schemes.

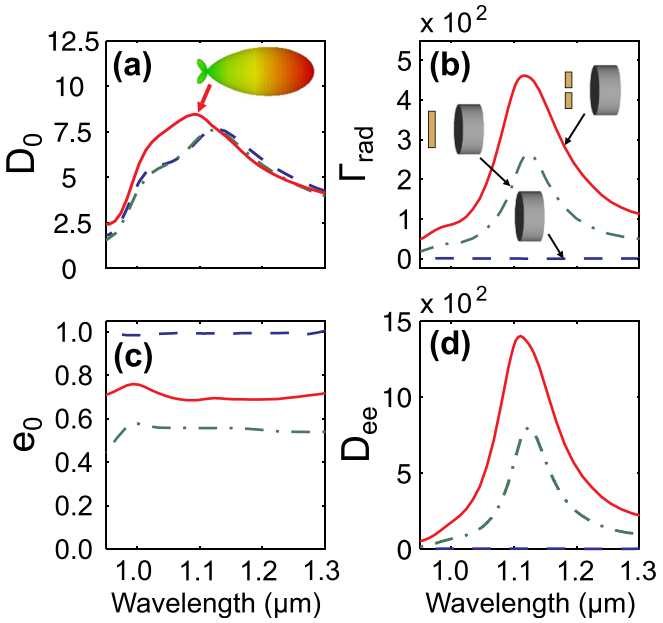

FIG. 4. Comparison of an all-dielectric (blue), a single rod hybrid (green), and a two rod hybrid (red) nanoantenna at an optimal separation d of 80 nm: (a) Directivity in the forward direction D_0, (b) radiative decay rate enhancement Γ_{rad}, (c) radiation efficiency e_0, and (d) directional emission enhancement D_{ee}. The insets in (a) and (b) show the emission pattern of the two rod hybrid nanoantenna at the position indicated by the arrows and schematics of the considered designs (not to scale), respectively.

The authors acknowledge a support from the Australian Research Council.

[1]P. Biagioni, J.-S. Huang, and B. Hecht, Rep. Prog. Phys. **75**, 024402 (2012).
[2]T. H. Taminiau, F. D. Stefani, and N. F. van Hulst, Opt. Express **16**, 10858 (2008).
[3]A. G. Curto, G. Volpe, T. H. Taminiau, M. P. Kreuzer, R. Quidant, and N. F. van Hulst, Science **329**, 930 (2010).
[4]G. Rui, R. L. Nelson, and Q. Zhan, Opt. Lett. **36**, 4533 (2011).
[5]I. S. Maksymov, I. Staude, A. E. Miroshnichenko, and Yu. S. Kivshar, Nanophotonics **1**, 65 (2012).
[6]I. M. Hancu, A. G. Curto, M. Castro-López, M. Kuttge, and N. F. van Hulst, Nano Lett. **14**, 166 (2014).
[7]F. B. Arango, A. Kwadrin, and A. F. Koenderink, ACS Nano **6**, 10156 (2012).
[8]M. Müller, S. Bounouar, K. D. Jöns, M. Glässl, and P. Michler, Nature Photon. **8**, 224 (2014).
[9]L. Zou, W. Withayachumnankul, C. M. Shah, A. Mitchell, M. Bhaskaran, S. Sriram, and C. Fumeaux, Opt. Express **21**, 1344 (2013).
[10]A. E. Krasnok, C. R. Simovski, P. A. Belov, and Yu. S. Kivshar, Nanoscale **6**, 7354 (2014).
[11]A. E. Krasnok, A. E. Miroshnichenko, P. A. Belov, and Yu. S. Kivshar, Opt. Express **20**, 20599 (2012).
[12]S. Person, M. Jain, Z. Lapin, J. J. Sáenz, G. Wicks, and L. Novotny, Nano Lett. **13**, 1806 (2013).
[13]I. Staude, A. E. Miroshnichenko, M. Decker, N. T. Fofang, S. Liu, E. Gonzales, J. Dominguez, T. S. Luk, D. N. Neshev, I. Brener, and Yu. S. Kivshar, ACS Nano **7**, 7824 (2013).
[14]G. Pellegrini, G. Mattei, and P. Mazzoldi, ACS Nano **3**, 2715 (2009).
[15]A. Devilez, B. Stout, and N. Bonod, ACS Nano **4**, 3390 (2010).
[16]B. Rolly, B. Stout, and N. Bonod, Opt. Express **20**, 20376 (2012).

[17]X. Zeng, W. Yu, P. Yao, Z. Xi, Y. Lu, and P. Wang, Opt. Express **22**, 14517 (2014).
[18]L. Rogobete, F. Kaminski, M. Agio, and V. Sandoghdar, Opt. Lett. **32**, 1623 (2007).
[19]P. B. Johnson and R. W. Christy, Phys. Rev. B **6**, 4370 (1972).
[20]*Handbook of Optical Constants of Solids*, edited by E. D. Palik (Academic Press, New York, 1985).
[21]P. Anger, P. Bharadwaj, and L. Novotny, Phys. Rev. Lett. **96**, 113002 (2006).
[22]C. A. Balanis, *Antenna Theory* (John Wiley & Sons, Inc., 2005).
[23]P. Grahn, A. Shevchenko, and M. Kaivola, New J. Phys. **14**, 093033 (2012).
[24]T. G. Habteyes, I. Staude, K. E. Chong, J. Dominguez, M. Decker, A. E. Miroshnichenko, Yu. S. Kivshar, and I. Brener, ACS Photonics **1**, 794 (2014).
[25]W. Liu, J. Zhang, B. Lei, H. Ma, W. Xie, and H. Hu, Opt. Express **22**, 16178 (2014).